Blind PAPR Reduction and ICA Based Equalization for mmWave FBMC-OQAM Systems

Ruixue Liu†, Xu Zhu*, Yufei Jiang†, Xiaojie Dong† and Fuchun Zheng†
* Department of Electrical Engineering and Electronics, University of Liverpool, Liverpool, UK
† School of Electronic and Information Engineering, Harbin Institute of Technology, Shenzhen, China
Emails: {liuruixue,dongxiaojie}@stu.hit.edu.cn, {xuzhu, fzheng}@ieee.org, jiangyufei@hit.edu.cn

***Abstract*— We propose a blind selective mapping (BSLM) based peak-to-average power ratio (PAPR) reduction method and an independent component analysis (ICA) based channel equalization structure for millimeter wave (mmWave) filter bank multi-carrier (FBMC) with offset quadrature amplitude modulation (OQAM) systems. On the one hand, a new phase adjustment factor is introduced in the BSLM based PAPR reduction scheme, which is spectrum-efficient as the phase ambiguity incurred can be resolved blindly at the receiver, requiring no side information. On the other hand, we propose an ICA based blind equalization scheme with a new phase shift correction approach, which can resolve the phase ambiguity incurred by ICA equalization. Simulation results show that the proposed structure can provide bit error rate (BER) performance close to zero-forcing (ZF) equalization with perfect channel state information (CSI), and the BSLM based PAPR reduction outperforms the existing methods in the literature, while requiring no side information at the receiver.**

***Index Terms*— Filter bank multi-carrier (FBMC), orthogonal quadrature amplitude modulation, (OQAM),peak-to-average power ratio (PAPR), independent component analysis (ICA)**

I. Introduction

Orthogonal frequency division multiplexing (OFDM) technique is robust against multipath fading and has been employed in long time evolution-advanced (LTE-Advanced) [1], [2]. However, there are a number of problems such as high out-of-band emissions (OOBE) and sensitivity to carrier frequency offset (CFO) in OFDM systems, which causes inter-carrier interference (ICI). To overcome the shortcomings of OFDM systems, filter bank multi-carrier with offset quadrature amplitude modulation (FBMC-OQAM) is considered as a promising candidate solution for future wireless communication systems, as the effect of ICI is reduced [3]. Because of no longer using cyclic prefix (CP), the FBMC-OQAM system provides spectral efficiency higher than OFDM systems. The utilization of millimeter wave (mmWave) communications can enable extremely high data rates and much richer multimedia services for future wireless systems [4]. Therefore, employing the CP-free FBMC-OQAM technique for mmWave can further improve the spectral efficiency. However, there is little work as such in the existing literature.

High peak-to-average power ratio (PAPR) is one of problems for mmWave FBMC-OQAM systems [5]. The high PAPR requires complex analogue-to-digital convertor (ADC) and digital-to-analogue convertor (DAC) to meet the high peak power of signals. Also, the high PAPR is limited to the battery life of power-limited devices. Therefore, it is crucial to reduce PAPR at the transmitter. In [6], extended selective mapping (ESLM) based PAPR reduction scheme was proposed for multiple-input multiple-output (MIMO) OFDM systems. The PAPR reduction performance degrades because of using the same phase adjustment factors on all the symbols in each subblock. Also, there are a number of PAPR reduction approaches for FBMC-OQAM systems in the literatures [7]-[9]. In [7], a clipping based PAPR reduction scheme was proposed for FBMC-OQAM systems. However, it causes in-band signal distortion and out-of-band radiation. In [8], a joint optimization scheme of partial transmit sequence (PTS) and clipping was proposed to mitigate the signal distortion in the PAPR reduction for FBMC-OQAM signals. In [9], the multi-block joint optimization based PTS was proposed to reduce the combined effect of the high PAPR and ICI in FBMC-OQAM systems. Nevertheless, the aforementioned schemes for PAPR reduction require heavy side information leading to spectral inefficiency.

Channel estimation and equalization play important roles for mmWave FBMC-OQAM systems [10], [11]. Blind or semi-blind approaches can enhance the spectral efficiency as a large number of training data are not required to estimate the channel state information (CSI). Independent component analysis (ICA), an effective higher order statistics (HOS) based blind source separation technique, is robust against Gaussian noise compared to the second order statistics (SOS) based methods [12], [13]. In [14], a blind OFDM receiver structure was proposed for ICA based MIMO systems. However, the error propagations exist. In [15], [16], a small number of pilots were used to eliminate the phase and permutation ambiguity in the ICA based equalization. In [6], a non-redundant linear precoding scheme was designed to eliminate the ambiguity for ICA based MIMO OFDM systems. However, the ambiguity elimination solutions above are designed for quadrature phase shift keying (QPSK) or binary phase shift keying (BPSK) modulation, and are not

suitable for FBMC systems with OQAM modulation. To the best of the authors' knowledge, there is no work to employ ICA for mmWave FBMC-OQAM systems in the literature.

In this paper, we propose a novel blind selective mapping (BSLM) based PAPR reduction scheme and an ICA based blind equalization structure for mmWave FBMC-OQAM systems. The contributions of this paper can be summarized as follows. First, the proposed BSLM PAPR reduction scheme is performed by introducing a new phase adjustment factor at the transmitter. The phase ambiguity incurred by the BSLM PAPR reduction scheme is resolved blindly at the receiver for mmWave FBMC-OQAM systems. Second, to the best of the authors knowledge, this is the first work to apply ICA for blind equalization in mmWave FBMC-OQAM systems. A new phase correction process is proposed to solve the phase shifting problem in the ICA equalized FBMC-OQAM signals. Third, the whole FBMC-OQAM system is spectrum-efficient, as no training sequence is required at the transmitter. Simulation results show that the proposed structure provides bit error rate (BER) performance close to zero-forcing (ZF) equalization with perfect channel state information (CSI), and the complementary cumulative distribution function (CCDF) performance of the PAPR reduction is better than that of the ELSM based PAPR reduction method [6], while requiring no side information.

II. System model

We consider a mmWave FBMC-OQAM system with P OQAM blocks consisting of M subcarriers each, as shown in Fig. 1. For mmWave systems, the signal propagation is dominated by line-of-sight (LOS) links. Motivated by the mentioned considerations, the channel can be modeled by a Rician multipath fading [17]. The transmitted OQAM symbol on subcarrier m $(m = 0, \ldots, M-1)$ in the i-th $(i = 0, \ldots, P-1)$ block can be expressed as

$$x(m,i) = u(m,i)\theta(m,i) \tag{1}$$

where $\theta(m,i) = j^{m+i}$ denotes the phase term on subcarrier m in the i-th block and $u(m,i)$ denotes the symbol pre-processed by precoding and PAPR reduction on the m-th subcarrier in the i-th OQAM block.

The synthesis filter bank (SFB) and analysis filter bank (AFB) are used to implement the modulator and demodulator of communication links, respectively. By using SFB, OOBE can be reduced significantly. The output signal of SFB is given by

$$\breve{x}(m,i) = G(m)x(m,i) \tag{2}$$

where $G(m) = \sum_{l=0}^{M-1} B(m)[\mathbf{W}]_{m,l}[p(m)]_{\uparrow \frac{M}{2}}$ [18] denotes the m-th synthesis filter with $B(m) = \exp\left(-j\frac{2\pi m}{M}\left(\frac{L_p-1}{2}\right)\right)$ being a multiplier to force the real-valued prototype pulse to be causal and L_p being the length of the prototype filter. $\mathbf{W}$ is the $M \times M$ inverse fast fourier transform (IFFT) matrix with (k,l) entry $[\mathbf{W}]_{k,l} = \exp\left(j\frac{2\pi kl}{M}\right)$. $p(m)$ is the PHYDYAS prototype filter with $\{\cdot\}_{\uparrow \frac{M}{2}}$ denoting the interpolation operation by a factor of $\frac{M}{2}$.

The efficient implementation of AFB at the receiver is matched to SFB at the transmitter. Hence, the m-th analysis filter can be expressed as $G^*(m)$ with superscript $*$ denoting the complex conjugate. The real orthogonality condition of FBMC-OQAM is $\Re\{G^*(m)G(m)\} = 1$ [19]. Thus, the channel induced ICI and inter-symbol interference (ISI) can be neglected according to [17]. Therefore, the output signal of AFB denoted by $y(m,i)$ on subcarrier m in i-th OQAM block can be expressed as

$$\begin{aligned} y(m,i) &= G^*(m)H(m)G(m)x(m,i) + z(m,i) \\ &= H(m)x(m,i) + z(m,i) \end{aligned} \tag{3}$$

where $H(m)$ is the channel frequency response on subcarrier m. $|H(m)| \sim \text{Rice}(\sqrt{\frac{K}{K+1}}, \frac{1}{\sqrt{2(K+1)}})$, where K is the Rician factor. $z(m,i)$ denotes the additive white Gaussian noise (AWGN) with a zero mean and a variance of $\frac{1}{2}\sigma_z^2$.

III. Precoding

A non-redundant linear precoding is used at the transmitter for both ICA equalization and PAPR reduction. On the one hand, the precoding can eliminate the phase ambiguity incurred by ICA equalization. On the other hand, a phase adjustment is introduced into the precoding to reduce the PAPR. The non-redundant linear precoding at the transmitter is shown as follows:

$$u(m,i) = \frac{1}{\sqrt{1+a^2}} q(m)[d(m,i) + a d_{\text{ref}}(m,i)] \tag{4}$$

where $d(m,i)$ denotes the real pulse amplitude modulation (PAM) symbol on subcarrier m in the i-th block, and $d_{\text{ref}}(m,i)$ denotes a pre-designed reference data known to the receiver. $a \in (0,1)$ is the real-valued precoding constant to give a tradeoff of power allocation between the source data $d(m,i)$ and the reference data $d_{\text{ref}}(m,i)$, and $q(m) \in \left\{e^{j\phi}, \phi \in (0, \frac{\pi}{2})\right\}$ is the phase adjustment factor on the m-th subcarrier to give a tradeoff between CCDF performance of PAPR reduction and BER performance of equalization. OQAM is not sensitive to phases, when $\phi \in (0, \frac{\pi}{2})$. As ϕ increases, the CCDF performance of PAPR reduction will improve. Meanwhile, BER performance will be worse, because the phase adjustment leads to error propagation. The selection of precoding constant a also provides a tradeoff between BER and CCDF performance. As a decreases, the influence of phase ambiguity incurred by precoding is little. Therefore, we formulate an objective function J subject to a, ϕ expressed as

$$J = ce(a,\phi) + (1-c)f(\phi) \tag{5}$$

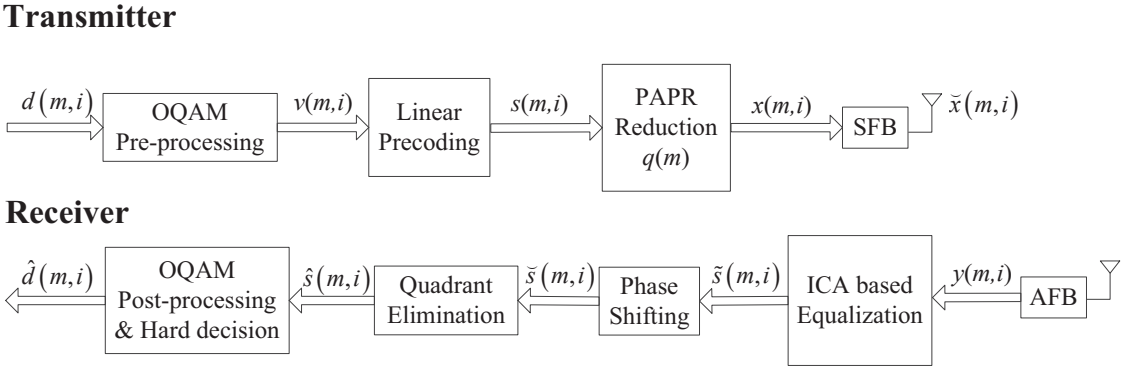

Fig. 1. Block diagram of the proposed FBMC-OQAM systems with PAPR reduction based on ICA equalization on subcarrier m and FBMC symbol i.

where $c \in [0,1]$ is the weight between BER and CCDF. $e(a,\phi)$ denotes BER influenced simultaneously by a, ϕ. $f(\phi)$ denotes CCDF influenced by ϕ. The selection of a and ϕ can be obtained by minimizing the objective function in Eq (5) expressed as

$$\begin{aligned} &[\hat{a},\hat{\phi}] = \arg\min_{\tilde{a},\tilde{\phi}} J \\ &\text{s.t. } 0 < \tilde{a} < 1, \\ &\quad 0 < \tilde{\phi} < \frac{\pi}{2} \end{aligned} \tag{6}$$

where $\tilde{a}$, $\tilde{\phi}$ are different values of a and ϕ. $\hat{a}$ and $\hat{\phi}$ are the optimal selection of a and ϕ.

IV. PAPR REDUCTION

As one of the conventional PAPR reduction schemes, SLM [20] requires side information, which leads to a spectral overhead. ESLM scheme [6] requires no side information as the phase ambiguity can be resolved together with the phase shifting in the ICA equalization at the receiver. However, the CCDF performance of ESLM is worse as the number of blocks increases. Hence, we propose a BSLM based PAPR reduction scheme by multiplying different symbols with different phase adjustment factors. The phase ambiguity incurred by the proposed PAPR reduction is eliminated blindly at the receiver. Therefore, the proposed method is spectrum-efficient, as no side information is required.

The process of the proposed BSLM is mainly implemented by utilizing the phase adjustment factor $q(m)$. In Fig. 2, the input symbol of PAPR reduction is $\mathbf{s}(i) = [s(0,i),\ldots,s(M-1,i)]$, with $s(t,i)$ denoting the SFB output continuous signal. The vector $\mathbf{q} = [q(0),\ldots,q(M-1)]$ denotes the phase adjustment vector and U denotes the maximum number of iterations. The PAPR of the i-th OQAM block is given by

$$\text{PAPR}\{\mathbf{s}(i)\} = \frac{\max\limits_{0\le t<T} |s(t,i)|^2}{\mathop{\text{E}}\limits_{t}\{|s(t,i)|^2\}} \tag{7}$$

where T denotes the period of a FBMC-OQAM block.

The detailed procedure of BSLM can be described as shown in Table I. In the iter-th (iter $= 1,\ldots,U$) iteration, $\mathbf{q}^{iter}$ denotes the phase adjustment factor of the iter-th iteration. $\mathcal{F}^{-1}\{\cdot\}$ denotes the IFFT process and L_s denotes the oversampling factor.

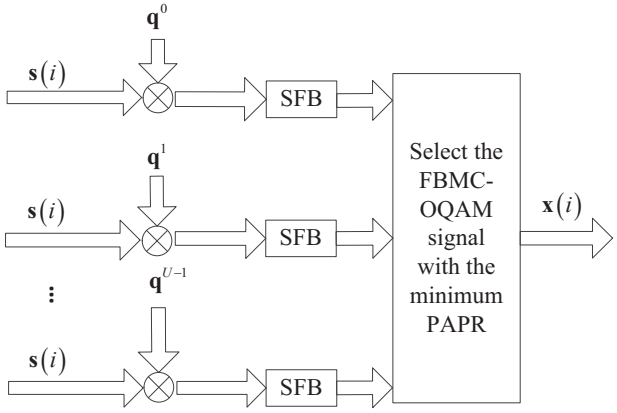

Fig. 2. Block diagram of blind selective mapping (BSLM) technique for PAPR reduction.

The output FBMC-OQAM signal $x(m,i)$ suffers from a phase shift $\Delta\phi(m,i)$ on subcarrier m in the i-th OQAM block denoted as follows:

$$\Delta\phi(m,i) = \text{angle}\{x(m,i)\} - \text{angle}\{s(m,i)\} \tag{8}$$

where angle$\{\cdot\}$ denotes the phase of a complex. From (8), we have $\Delta\phi(m,i) < \phi_{max}$, where ϕ_{max} is the maximum phase belonging to $(0, \frac{\pi}{2})$. The phase shift of $\Delta\phi(m,i)$ due to the PAPR reduction is introduced into received signals, and can be solved blindly via the OQAM demodulation for mmWave FBMC systems. Therefore, the proposed BSLM is spectrum-efficient, compared to traditional SLM, as the side information is not required.

TABLE I
BSLM ALGORITHM

Input

Initialize U and iter=1.

1. **While** iter $\leq U$
2. Randomly generate a vector
   $\boldsymbol{\phi} = \{\phi(0,i), \cdots, \phi(M-1,i)\}$, $\phi(m,i) \in (0, \frac{\pi}{2})$.
3. Calculate phase adjustment vector $\mathbf{q}^{iter}$=$e^{j\boldsymbol{\phi}}$.
4. Adjust phase $\mathbf{s}(i)\mathbf{q}^{iter}$.
5. Interpolation: $\{\mathbf{s}(i)\mathbf{q}^{iter}\}_{L_s\uparrow}$.
6. IFFT: $\mathcal{F}^{-1}\{\{\mathbf{s}(i)\mathbf{q}^{iter}\}_{L_s\uparrow}\}$.
7. Calculate PAPR:
8. $\max\limits_{0\leq t<T} |s(t,i)|^2$=max$\{\mathcal{F}^{-1}\{\{\mathbf{s}(i)\mathbf{q}^{iter}\}_{L_s\uparrow}\}\}$,
9. $\mathop{\mathrm{E}}\limits_{t}\{|s(t,i)|^2\}$=mean$\{\mathcal{F}^{-1}\{\{\mathbf{s}(i)\mathbf{q}^{iter}\}_{L_s\uparrow}\}\}$,
10. $\mathrm{PAPR}_{iter} = \frac{\max\limits_{0\leq t<T} |s(t,i)|^2}{\mathop{\mathrm{E}}\limits_{t}\{|s(t,i)|^2\}}$.
11. iter=iter+1.
12. **endwhile**
13. $\mathbf{q}^{opt}$=arg $\min\limits_{iter} \mathbf{s}(i)\mathbf{q}^{iter}$.
14. Calculate $\mathbf{x}(i) = \mathbf{s}(i)\mathbf{q}^{opt}$.

V. ICA BASED BLIND EQUALIZATION

As a robust HOS based blind source separation technique, ICA can be applied to the received signal $y(m,i)$ in order to recover the transmitted signals. Firstly, the whitening of the received signals are preprocessed. Then JADE [12], one of the ICA algorithms, requiring shorter data sequences than the other ICA methods, is applied. After using ICA, the equalized signal $\tilde{s}(m,i)$ can be written as [14]

$$\tilde{s}(m,i) = g(m)\Delta\phi(m,i)s(m,i) \tag{9}$$

where $g(m)$ on the m-th subcarrier denotes the phase ambiguity resulting from ICA equalization. Due to this phase ambiguity, $\tilde{s}(m,i)$ will have different phase shifts compared to the original source stream $s(m,i)$.

In order to handle the phase ambiguity existed in the ICA equalized signal $\tilde{s}(m,i)$, the de-rotation operation for the transmitted signal can be expressed as

$$\breve{s}(m,i) = \tilde{s}(m,i)[\alpha(m)/|\alpha(m)|] \tag{10}$$

where the rotation factor $\alpha(m)$ is used to correct the phase deviation. The existing work about the phase shifting process is based on BPSK or QPSK modulation [14]. However, in mmWave FBMC-OQAM systems, OQAM modulation is used to eliminate the ICI. To the authors' best knowledge, there is no work about OQAM based phase shifting process. Therefore, the proposed OQAM based phase shifting process and $\alpha(m)$ for OQAM modulation can be derived as

$$\alpha(m) = \left\{ \frac{1}{P} \sum_{i=1}^{P-1} [\tilde{s}(m,i)]^4 \right\}^{-\frac{1}{4}} \tag{11}$$

However, the phase shifting process introduces quadrant ambiguity represented by $b(m) = \frac{\pi}{2}l$ $(l \in \{0,1,2,3\})$. Hence, the output signal $\breve{s}(m,i)$ after phase shifting can be expressed as

$$\breve{s}(m,i) = b(m)s(m,i) \tag{12}$$

In order to further eliminate the quadrant ambiguity generated by phase shifting, ρ is defined as the cross-correlation between the detected symbols and the reference symbols on subcarrier m in i-th OQAM block as follows:

$$\rho = \frac{1}{P} \sum_{i=0}^{P-1} \breve{s}(m,i)[v_{\mathrm{ref}}(m,i)]^* \tag{13}$$

where $v_{\mathrm{ref}}(m,i)$ is the OQAM modulated reference data.

Then, $b(m)$ is defined as the combined phase shifts introduced by both ICA equalization and PAPR reduction, which is given by

$$b(m) = \left[e^{-j\frac{\pi}{4}} \mathrm{sign}\left(\frac{\rho}{|\rho|} e^{-j\frac{\pi}{4}} \right) \right]^{-1} \tag{14}$$

Therefore, the estimated data $\hat{s}(m,i)$ after quadrant elimination can be obtained as

$$\hat{s}(m,i) = \frac{\breve{s}(m,i)}{b(m,i)} \tag{15}$$

Next, only the process of hard decision is employed to get the hard estimate $\hat{d}(m.i)$ of the source data $d(m.i)$ with the quadrant ambiguity eliminated. Due to OQAM modulation, $\Delta\phi(m,i)$ can be solved blindly at the receiver.

VI. SIMULATION RESULTS

In this section, simulation results are produced to illustrate the CCDF performance of the proposed BSLM algorithm and the BER performance of ICA equalization for mmWave FBMC-OQAM systems. CCDF is defined as the probability that the PAPR exceeds a specific value γ, which can be denoted by CCDF = Pr(PAPR $> \gamma$). The number of subcarriers used is $M = 64$ and the number of FBMC-OQAM blocks is $P = 256$. The frequency used for mmWave is 60 GHz. Besides, 4 QAM modulation is used in the mmWave FBMC-OQAM systems with the overlapping factor $L_{\mathrm{o}} = 4$. Hence, the length of the prototype filter is $L_{\mathrm{p}} = L_{\mathrm{o}}M - 1 = 255$. We employed the Rician multipath fading channel model with the root mean square (RMS) delay of 46 ns and the Rician factor $K = 5$ for mmWave at 60 GHz. The predefined precoding constant is $a = 0.25$, obtained by implementing plenty of experiments. For PAPR reduction, the oversampling factor is $L_{\mathrm{s}} = 4$ and the maximum number of iterations is $U = 16$.

Fig. 3 shows the CCDF performance of PAPR for the proposed BSLM scheme compared with the ESLM scheme [6] for mmWave FBMC-OQAM systems. Apparently, the proposed BSLM scheme outperforms the ESLM scheme [6] with the same calculation complexity. ESLM has an obvious PAPR reduction when $\gamma > 9.5$. However, as $\gamma > 6$, the proposed BSLM scheme can obtain a significant reduction. At CCDF $= 10^{-2}$, the PAPR reduction using BSLM scheme for mmWave FBMC-OQAM systems is about 1 dB better than that of the ESLM scheme.

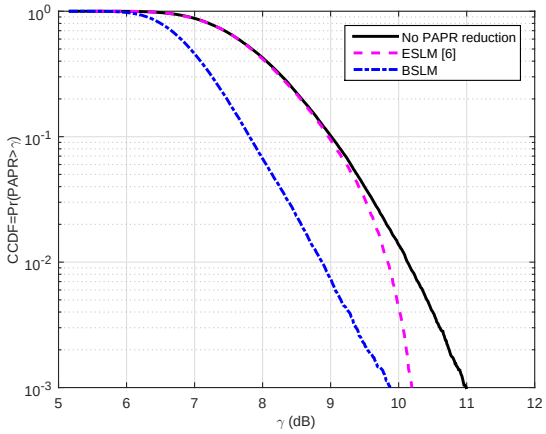

Fig. 3. CCDF performance of BSLM PAPR reduction scheme for mmWave FBMC-OQAM system with the OQAM block length $P = 256$, $M = 64$ subcarriers, the precoding constant $a = 0.25$ and the phase term $\phi = \frac{\pi}{3}$.

Fig. 4 shows the impact of phase ϕ on CCDF perfomance of BSLM based PAPR reduction for mmWave FBMC-OQAM system. At different of 7,8,9 dB, the trend of CCDF performances is similar. As $\phi \in (0, \frac{\pi}{2})$ increases, the CCDF performance of the proposed PAPR reduction will improve. The reason is that there is a large range of phase offsets, leading to the high possibility of peak power reduction.

Fig. 5 shows the BER performance of the ICA equalization based mmWave FBMC-OQAM systems compared with that of ZF equalization with perfect CSI. We employ a precoding constant of $a = 0.25, 0.45$ and 0.75. It can be concluded that when $P = 256$ and $a = 0.25$, ICA equalization can provide an approximate performance to the ZF equalization with the perfect CSI. Besides, the BER performance of ICA equalization at $a = 0.45$ is close to that of ICA equalization at $a = 0.25$. Therefore, we can adjust a to obtain the optimal performance of ICA equalization for mmWave FBMC-OQAM systems.

Fig. 6 shows the impact of phase ϕ on BER perfomance of BSLM based PAPR reduction for mmWave FBMC-OQAM system. When signal-to-noise ratio (SNR) equals to 20 dB and 30 dB, the BER performance is worse as ϕ increases for both OFDM and FBMC-OQAM systems. The impact of BSLM based PAPR reduction is little when $\phi \in (0, \frac{\pi}{3})$. However, as shown in Fig. 4, the CCDF performance improves as ϕ increases. Therefore, there is a tradeoff between BER and CCDF performances.

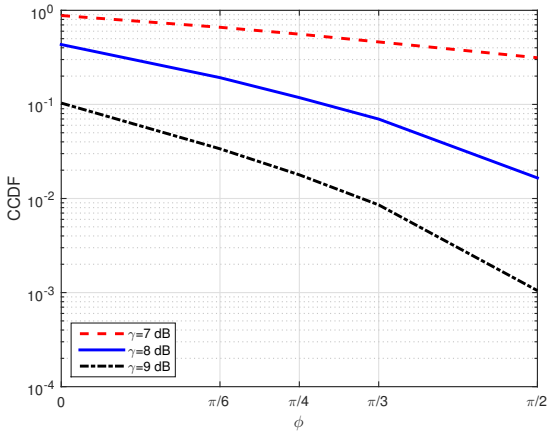

Fig. 4. Impact of phase ϕ on CCDF perfomance of BSLM based PAPR reduction for mmWave FBMC-OQAM system with the OQAM block length $P = 256$, $M = 64$ subcarriers and the precoding constant $a = 0.25$.

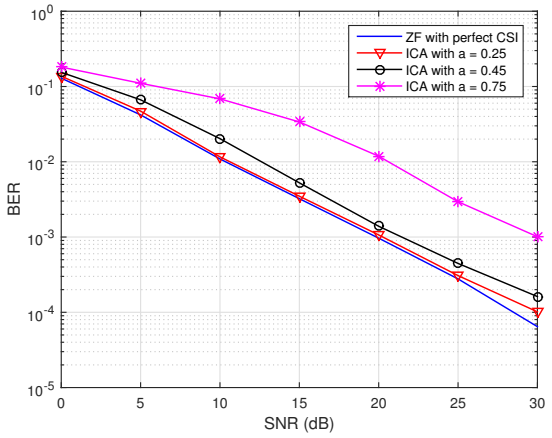

Fig. 5. BER performance of ICA based mmWave FBMC-OQAM system with BSLM PAPR reduction scheme for the OQAM block length $P = 256$, $M = 64$ subcarriers and the precoding constant $a = 0.25$.

VII. CONCLUSION

In this paper, a novel BSLM based PAPR reduction scheme and an improved ICA based blind equalization structure have been proposed for the mmWave FBMC-OQAM systems. The

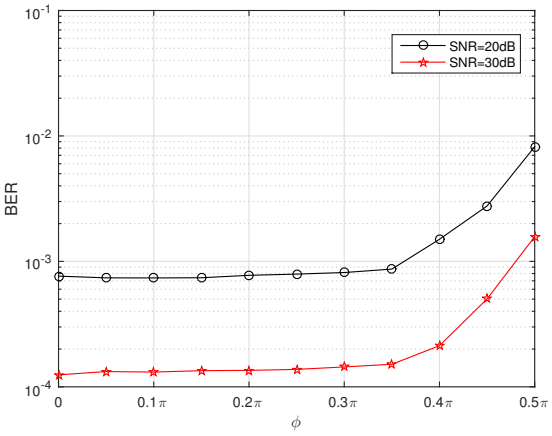

Fig. 6. Impact of phase ϕ on BER perfomance of the BSLM based PAPR reduction for mmWave FBMC-OQAM system with $M = 64$ subcarriers and the precoding constant $a = 0.25$.

phase ambiguity incurred by BSLM can be solved blindly at the receiver, and no side information is required. Also, an OQAM based phase shifting process was proposed for the ICA based FBMC-OQAM systems. The simulation results demonstrated that the ICA based receiver can provide a close BER performance to the ZF based receiver with perfect CSI. Furthermore, the proposed BSLM scheme can significantly reduce the PAPR compared with the ESLM scheme [6] and further enhance the spectral efficiency in the mmWave FBMC-OQAM systems.

VIII. Acknowledgments

This work was supported in part by the Science and Technology Innovation Commission of Shenzhen under Project No. JCYJ20170307151258279.

References

[1] T. Hwang, C. Yang, G. Wu, S. Li, and G. Y. Li, "OFDM and its wireless applications: a survey," *IEEE Trans. Veh. Tech.*, vol. 58, no. 4, pp. 1673-1694, May 2009.

[2] Y. Jiang, Y. Wang, P. Cao, M. Safari, J. Thompson, and H. Haas, "Robust and low-complexity timing synchronization for DCO-OFDM LiFi systems," *IEEE J. Sel. Areas Commun.*, vol. 36, no. 1, pp. 53-65, Jan. 2018.

[3] T. Ihalainen, A. Ikhlef, J. Louveaux, and M. Renfors, "Channel equalization for multi-antenna FBMC/OQAM receivers," *IEEE Trans. on Veh. Tech.*, vol. 60, no. 5, pp. 2070-2085, Jun. 2011.

[4] Z. Wei, X. Zhu, S. Sun, and Y. Huang, "Energy-efficiency-oriented cross-layer resource allocation for multiuser full-duplex decode-and-forward indoor relay systems at 60 GHz," *IEEE J. Sel. Areas Commun.*, vol. 34, no. 12, pp. 3366-3379, Dec. 2016.

[5] A. Skrzypczak, P. Siohan, and J. P. Javaudin, "Analysis of the peak-to-average power ratio for OFDM/OQAM," in *Proc. IEEE Signal Process. Advan. Wireless Commun.*, pp. 1-5, Jul. 2006.

[6] J. Gao, X. Zhu, and A. K. Nandi, "Non-redundant precoding and PAPR reduction in MIMO OFDM systems with ICA based blind equalization," *IEEE Trans. Wireless Commun.*, vol. 8, no. 6, pp. 3038-3049, Jun. 2009.

[7] Z. Kollar, L. Varga, and K. Czimer, "Clipping-based iterative PAPR-reduction techniques for FBMC," in *Proc. IEEE 17th InOWo*, pp. 1-7, Aug. 2012.

[8] J. Zhao, S. Ni, and Y. Gong, "Peak-to-average power ratio reduction of FBMC/OQAM signal using a joint optimization scheme," *IEEE Access*, vol. 5, pp. 15810-15819, May 2017.

[9] D. Qu, S. Lu, and T. Jiang, "Multi-block joint optimization for the peak-to-average power ratio reduction of FBMC-OQAM signals," *IEEE Trans. Signal Process.*, vol. 61, no. 7, pp. 1605-1613, Apr. 2013.

[10] X. Ma, F. Yang, S. Liu, J. Song, and Z. Han, "Design and optimization on training sequence for mmWave communications: a new approach for sparse channel estimation in massive MIMO," *IEEE J. Sel. Areas Commun.*, vol. 35, no. 7, pp. 1486-1497, Jul. 2017.

[11] M. Fuhrwerk, S. Moghaddamnia, and J. Peissig, "Scattered pilot-based channel estimation for channel adaptive FBMC-OQAM systems," *IEEE Trans. on Wireless Commun.*, vol. 16, no. 3, pp. 1687-1702, Mar. 2017.

[12] J. F. Cardoso, "High-order contrasts for independent component analysis," *Neural Comput.*, vol. 11, pp. 157-192, Jan. 1999.

[13] Y. Jiang, X. Zhu, E. Lim, Y. Huang, and H. Lin, "Low-complexity semiblind multi-CFO estimation and ICA-based equalization for CoMP OFDM systems," *IEEE Trans. Veh. Tech.*, vol. 63, no. 4, pp.1928-1934, May 2014.

[14] L. Sarperi, X. Zhu, and A. K. Nandi, "Blind OFDM receivers based on independent component analysis for multiple-input multiple-output systems," *IEEE Trans. on Wireless Commun.*, vol. 6, no. 11, pp. 4079-4089, Nov. 2007.

[15] Z. Ding, T. Ratnarajah, and C. Cowan, "HOS-based semi-blind spatial equalization for MIMO Rayleigh fading channels," *IEEE Trans. on Signal Process.*, vol. 56, no. 1, pp. 248-255, Jan. 2008.

[16] L. Sarperi, X. Zhu, and A. K. Nandi, "Semi-blind space-time equalization for single-carrier MIMO systems with block transmission," in *Proc.14th Eur. Signal Process.*, pp. 1-5, Sep. 2006.

[17] R. Nissel, E. Zöchmann, M. Lerch, S. Caban, and M. Rupp, "Low-latency MISO FBMC-OQAM: it works for millimeter waves!," in *Proc. 2017 IEEE Int. Microw. Symp.*, pp. 673-676, Jun. 2017.

[18] M. Bellanger, FBMC physical layer: a primer, PHYDYAS FP7 project document, Jan. 2010. [Online]. Available: http://www.ict-phydyas.org/teamspace/internal-folder/special-session-at-crowncom-2010

[19] R. Nissel, S. Schwarz, and M. Rupp, "Filter bank multicarrier modulation schemes for future mobile communications," *IEEE J. Sel. Areas Commun.*, vol. 35, no. 8, pp. 1768-1782, Aug. 2017.

[20] T. Jiang and Y. Wu, "An overview: peak-to-average power ratio reduction techniques for OFDM signals," *IEEE Trans. Broadcast.*, vol. 54, no. 2, pp. 257-268, Jun. 2008.